J. E. Davies

Control of Magnetic Properties During the Processing of Single Crystal Garnet Films

Abstract: Thin single-crystal rare earth iron garnet films are currently the most attractive materials for magnetic bubble domain applications. To utilize their potential, tight control of the magnetic properties is needed at each of the film processing steps. Such steps include the growth of large-area films from a supersaturated $PbO\text{-}B_2O_3$ fluxed melt, the phosphoric acid trimming of as-grown films to adjust the bubble collapse field, ion implantation of the film surface to suppress the formation of hard bubbles and the subsequent annealing the implanted layer receives during the thermal cycling of the device fabrication steps. Control of film properties at each of these stages will be discussed and data presented to show how each of these stages may be optimized.

Introduction

To develop mass memories based on magnetic bubble domains it is necessary to have large-area, highly perfect magnetic garnet films with closely matching properties, particularly with regard to the bubble collapse field H_0, the demagnetized stripewidth S_w and the film thickness h [1]. Because H_0 has the greatest impact on device operating margins, it is desirable to control its film-to-film variation to the tightest possible tolerances. Tight H_0 control minimizes the tedious task of sorting chips and matching them with the barium hexaferrite permanent magnet which provides the magnetic bias field in the packaged memory. Since h and S_w have a less direct effect on overlapping device operating margins, somewhat lower tolerances (as much as ± 10 percent) are often quoted. Although more than 90 percent of as-grown films meet the h and S_w tolerances, less than 50 percent fall within an H_0 tolerance of ± 1 percent.

Trimming of the film thickness with a phosphoric acid etch has been previously used as a post-growth method for adjusting H_0 for 6-μm bubble domains [2, 3]. Here results are presented to show that with some modification the same trimming technique works equally well for smaller bubbles. After trimming, the films are implanted with neon ions to suppress hard bubbles [4]. The useful range of implant conditions is defined and the effect of the implant on H_0 and S_w discussed. During subsequent processing steps the film is subjected to temperature cycles, which causes an anneal of the implanted layer. This further affects H_0. Direct measurements and independent annealing studies reveal that the magnitude of this effect depends on the conditions of the temperature cycle (time, temperature) and on the film implantation conditions.

Film growth

Garnet films for magnetic bubble domain applications are generally grown by the LPE (liquid phase epitaxy) method, which involves dipping a $Gd_3Ga_5O_{12}$ garnet substrate wafer into an isothermal supersaturated solution of the magnetic garnet in a $PbO\text{-}B_2O_3$ flux [5]. The substrate is usually rotated in a horizontal plane (≈ 100 rpm) to promote uniformity of thickness and magnetic properties across the diameter of the film [6]. Typical growth temperatures are ≈ 1223 K (950°C) and growth rates $\approx 1 \mu$m/min.

For processing economy it is clearly advantageous to use large-area magnetic garnet films. At present 5-cm (2″) diameter films are grown routinely in most facilities. With appropriate care H_0 can be maintained to within ± 1 percent across the film except for an $\approx$3-mm rim at the film periphery. Exploratory film depositions have also been made on 7.6-cm (3″) diameter substrates in our laboratory and have produced promising results (H_0 uniformity to ± 1 percent over 80 percent of useful film area) [7]. However, 7.6-cm technology is limited by the availability of good quality $Gd_3Ga_5O_{12}$ boules from which these large substrate wafers can be fabricated.

The factors that cause film-to-film variations in properties have been discussed in detail by Hewitt et al. [8], Stein [9], and Kasai and Ishida [10] for 6-μm bub-

bles and by Lewis [11] for 3-μm bubble films of the same compositions as those studied here (properties listed in Table 1). The same authors report empirical growth strategies whereby the film growth parameters (time, temperature, rotation rate) are adjusted from run to run to compensate for small, short-term drifts in film properties and additions of garnet/solvent are made to the LPE melt to compensate for the larger, long-term drifts that are encountered when growing many films.

Film trimming

Analyses of a number of films grown from different LPE furnaces show that although virtually all as-grown films fall within the S_w range of 3.0 ± 0.2 μm, less than 50 percent are within the film-to-film variation of ± 1 percent for H_0. Typically, the H_0 distribution has a standard deviation $\sigma \approx 143$ A $\cdot$ m^{-1} (1.8 Oe). Licht [2] and Kasai [3] have shown that phosphoric acid trimming of film thickness can be used as a post-growth method of controlling H_0 for 6-μm bubble films. An etch temperature of $\approx$443 K (170°C) was chosen by Licht since it is where phosphoric acid reaches a stable density. This gives etch rates of approximately 0.5 μm/min. The relationship between H_0 and h is given by [12]:

$$H_0 = 4\pi M\left(1 + \frac{3l}{4h} - \sqrt{\frac{3l}{h}}\right), \tag{1}$$

where l is the film characteristic length (a property of the material). Since $l < h$, H_0 decreases with decreasing h. Typically for compositions A and B (Table 1) the removal of 0.1 μm from the film thickness will decrease H_0 by $\approx$240 A $\cdot$ m^{-1} (3 Oe). In the region of interest,

$$S_w \approx 6l + 0.3h. \tag{2}$$

Consequently, a 0.1-μm reduction in h produces an approximately 0.03-μm reduction (i.e., 1 percent) in S_w. Since 1σ for as-grown films is about 143 A $\cdot$ m^{-1}, the effect of film etching on S_w is clearly small.

To utilize the trimming technique for 3-μm bubble films, the etch rate must be slowed down by using lower etch temperatures. This can be done with the 1:1 (by weight) phosphoric:sulphuric acid mixture developed by Reisman et al. [13] for chemical polishing of sapphire and spinel. This mixture is very stable over a wide temperature range and affords convenient film etch rates ($\approx$0.02 μm/min) at 401 K (128°C). To ensure reproducibility, good temperature control is needed since etch rate approximately doubles for each eight-degree temperature increase. Also the water content of the acid mixture must be controlled since water reduces the tendency of phosphoric acid to polymerize and thus increases the etch rate. Fortunately, the acid mixture stabilizes its water content at the etch temperature (Fig. 1). Provided we wait long enough (>24 hours) for

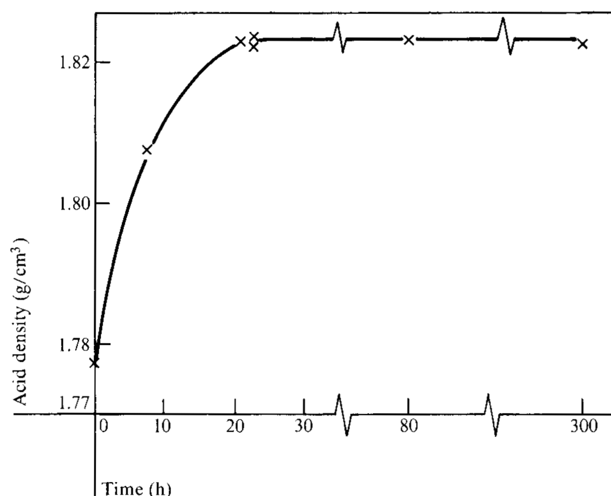

Figure 1 Density of etching acid vs time at 401 K (128°C).

Table 1 Garnet film properties.

Property	*Composition A*	*Composition B*
Formula	$(EuYTm)_3(FeGa)_5O_{12}$	$(SmYLuCa)_3(FeGe)_5O_{12}$
H_0(Oe)	120	140
H_0(A $\cdot$ m^{-1})	9600	11200
S_w(μm)	3.0	3.0
h(μm)	2.2	2.2
4πM(Gauss)	305	340
Wall energy, σ	0.29	0.36
Stability factor, Q	6.0	5.3

the acid to equilibrate, then reproducible film etching is a routine exercise.

Data for films of compositions A and B are given in Figs. 2 and 3, respectively. Using a combined strategy of aiming slightly for the thick side when growing films and then etching back, the yield of films to an H_0 tolerance of ± 1 percent improves to $\approx$90 percent. No degradation of film uniformity has been observed during etching.

A few additional points are worth mentioning:

1. The etching process is not, of course, limited to narrowing the H_0 distribution spread. It can be used to tailor the distribution shape as dictated by device packaging considerations.
2. Smaller bubbles require thinner films and larger 4πM. It becomes more difficult to control H_0 by the film growth process alone and so trimming is essential.
3. As-grown films usually have a nonuniform surface layer. Etching removes this layer and renders the film surface clean for ion implantation and subsequent processing.

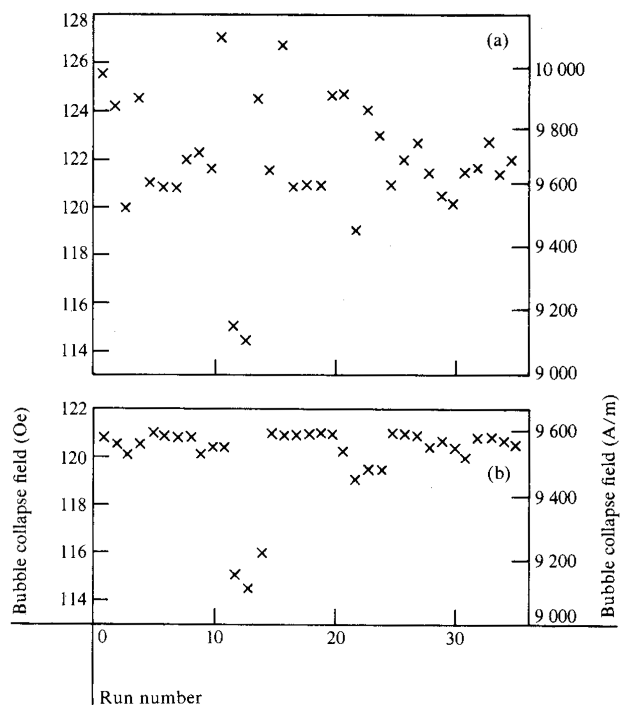

Figure 2 Effect of etching films of composition A. (a) As-grown films. (b) After etching.

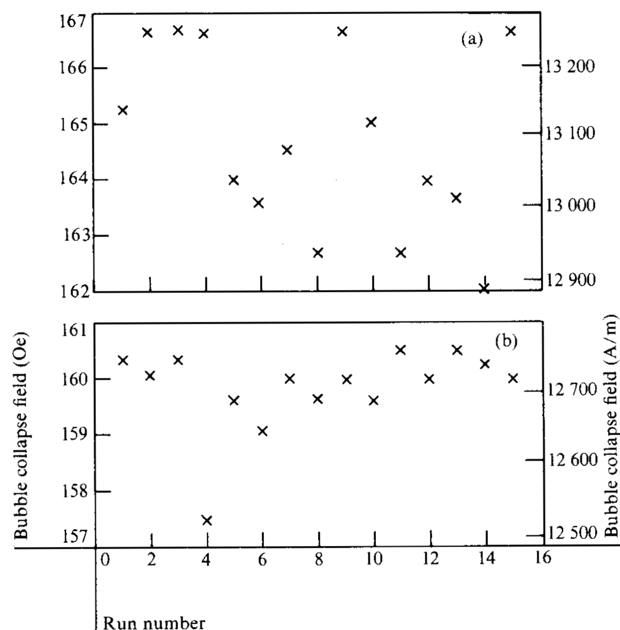

Figure 3 Effect of etching films of composition B. (a) As-grown films. (b) After etching.

Ion implantation

In garnet films, differences in the bubble domain wall structure give rise to a number of bubble "quantum states," each having its own characteristic static and dynamic properties. For successful operation of a field access (T-I or C-bar) device, one stable bubble state (the so-called soft bubble) is required. This can be achieved by ion implanting the film surface [4, 14]. The effect is to place the surface in a compression state relative to the bulk of the film. This, through magnetostriction, can cause the surface layer magnetization to fall into the plane of the film, forming a capping layer on the bubble (Fig. 4). With this configuration only one bubble state is stable under typical device operating conditions. The hard bubbles, which collapse at higher bias fields, are eliminated. Although hard bubble suppression has been demonstrated with a number of implanted species, neon ions are most commonly used because of the low dosages needed and consequently the short processing times ($\approx$3 minutes per film). The penetration depth of Ne^+ into the garnet lattice is $\approx$0.13 μm at 80 KeV and $\approx$0.18 μm at 120 KeV.

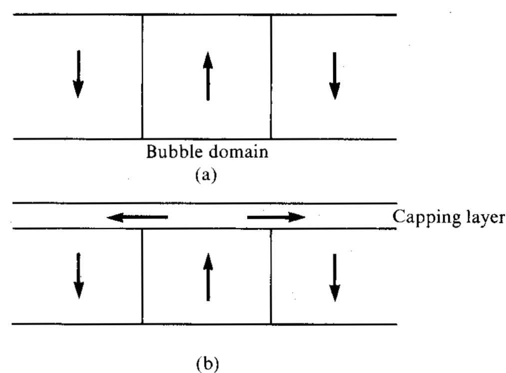

Figure 4 Ion implantation for hard bubble suppression. (a) As-grown film. (b) Ion-implanted film.

The effect of the Ne^+ dosage on film properties is shown in Fig. 5. As the dosage is increased to a level where the capping layer forms, H_0 increases due to the "keeper effect" (i.e., the capping layer allows a path of flux closure between the bubble and the surrounding domain of opposite polarity, thus increasing the bubble stability). At higher doses the cap becomes over-damaged, eventually to a point where hard bubble suppression is lost, and H_0 decreases below the preimplantation value due to a bubble shortening effect. For this material (composition B) the optimum implant dosage at 80 KeV is $\approx 1\text{-}2 \times 10^{14}$.

It is important to know the reproducibility of the ion-implantation effect. This is shown in Fig. 6 for implant conditions of 2×10^{14} at 120 KeV at normal incidence on composition B. Measurements of H_0 were made at 298 K (25°C) at the center of each film. The number of films implanted in each run is shown at the bottom of the bar which indicates the spread in ΔH_0 for all the films implanted in that run. It can be seen that from film to film and run to run the effect is reproducible. A further point is that all the implant runs were made using a beam

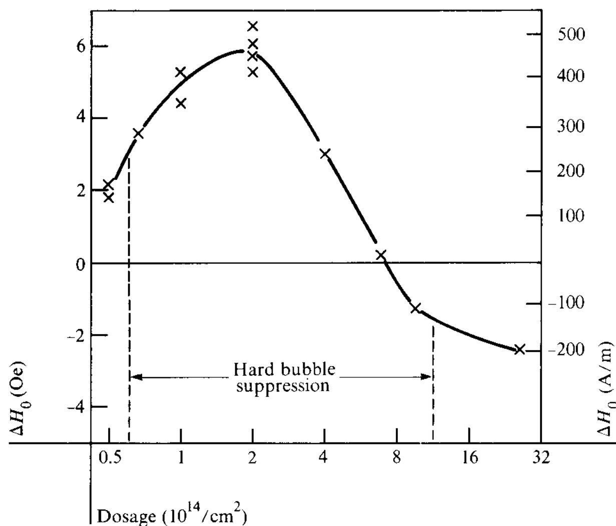

Figure 5 Effect of implant dosage (Ne^+/cm^2) at 80 KeV on collapse field change (ΔH_0) for composition B.

current of 10 μA (implant time $\approx$3 min) except for the data marked with an asterisk (*). Here the beam current was varied between 1 μA and 50 μA with corresponding implant times of 30 minutes to 0.6 minute. The ΔH_0 scatter over these ten implanted wafers is comparable with the scatter at constant beam current. This indicates that during implant the temperature at the film surface does not rise much above room temperature; otherwise there would have been appreciable ΔH_0 spread due to annealing effects.

In addition to causing the increase in H_0, implantation causes a decrease in the a.c. demagnetized S_w. For the films in Fig. 6 the average decrease is $\approx$6 percent. This is caused partly by the decrease in bubble height and partly by the decrease in energy of the domain wall immediately beneath the implanted layer.

Temperature effects

During device fabrication the films are submitted to a number of processing steps involving temperatures up to 673 K (400°C). Ordinarily, garnet is extremely stable, requiring temperatures above 1073 K (800°C) before any change in magnetic properties becomes measurable. However, ion implantation places the film surface in a state of high compressive strain and destroys some of the crystalline order, with the net result that annealing of the implanted layer can occur at low temperatures.

The results of annealing films of composition B in air are shown for three implant conditions in Fig. 7. Clearly the degree of annealing depends on the implant damage, which in turn depends on the implant dose and energy. Also the fact that the H_0 increase can be divided into two distinct regions, a rapid increase (occurring in <5

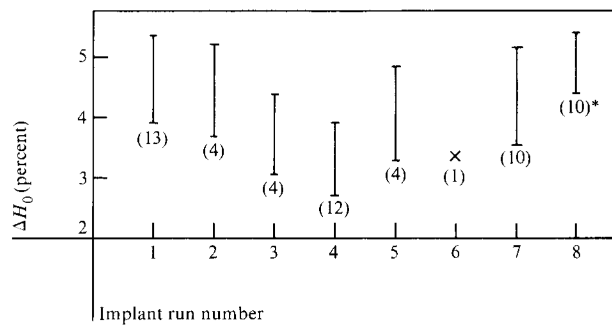

Figure 6 Reproducibility of implantation (120 KeV/2 × 10^{14}) for composition B. The height of the bars represents the range of ΔH_0 for the number of films (n) implanted in the same run.

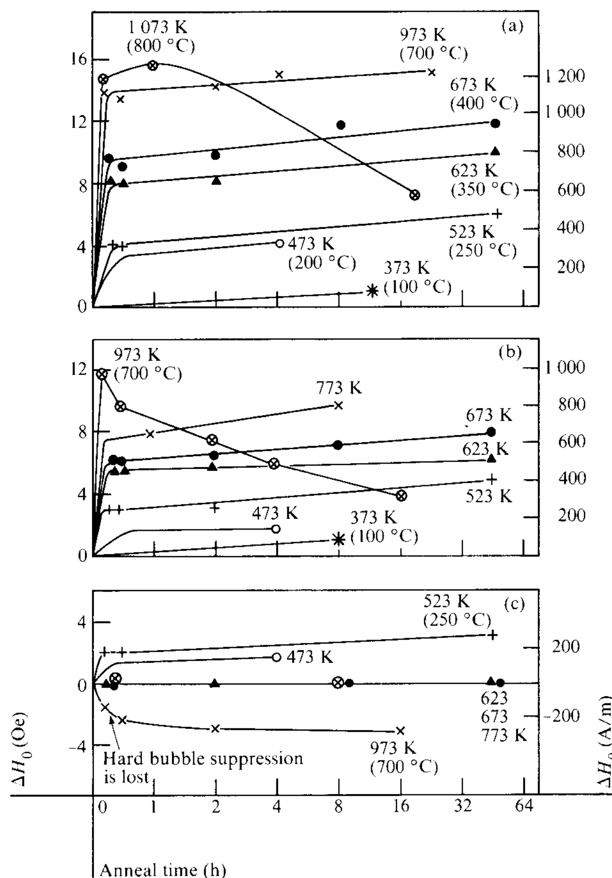

Figure 7 Effect on H_0 of annealing implanted films of composition B in air. Implant conditions are: (a) 120 KeV, 2 × 10^{14}. (b) 80 KeV, 2 × 10^{14}. (c) 80 KeV, 1 × 10^{14}.

minutes at temperatures above 673 K) followed by a slow rise to a plateau, which takes many hours to reach at a given temperature, indicates that the nature of the Ne^+ implant damage is complex and its annealing behavior cannot be explained by a single, thermally-activated process. Similar conclusions can be drawn from the data of Seman et al. [15], who used optical absorption to study ion-implanted garnet films.

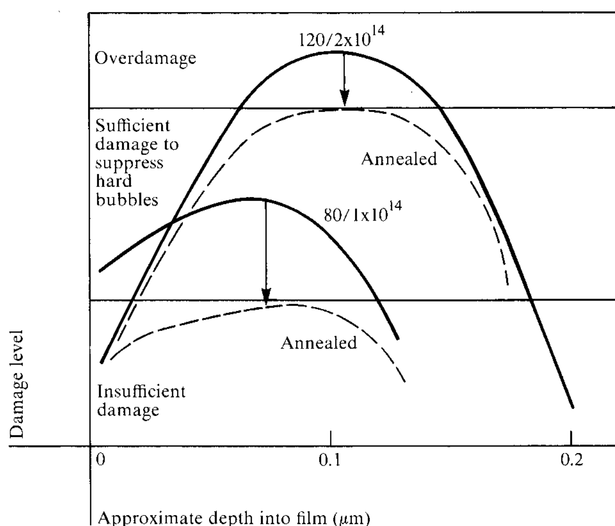

Figure 8 A model to explain the annealing data in terms of damage profiles.

It should be noted that the H_0 increase caused by annealing is in addition to the increase due to the initial implantation, indicating that the annealing causes a more effective capping layer. This is consistent with the results of Wolfe and North [16], who observed that annealing enhanced the formation of in-plane domains, as viewed by ferrofluid decoration, in the capping layer.

The differences in annealing characteristics for the three different implant conditions in Figs. 7(a), (b), and (c) are marked. For the $120/2 \times 10^{14}$ implant, the combined (implant plus anneal) increase is large and approaches the theoretical maximum that can be expected for composition B with a capping layer of $\approx$0.18 μm thickness. On the other hand, the $80/1 \times 10^{14}$ implant shows small or zero increase at low temperatures and readily loses the hard bubble suppression effect if the temperature exceeds 973 K for more than a few minutes.

Engemann and Hsu [17] have proposed the concept of a structured capping layer to explain the effect of Ne^+ implantation conditions on the minimum drive field to move a bubble. This concept also offers a qualitative explanation of the annealing data, as shown in Fig. 8. For the $80/1 \times 10^{14}$ implant, the damage just exceeds the minimum to suppress hard bubbles (see Fig. 5). Temperatures in excess of 973 K (700°C) readily reduce this damage level to below the minimum with a resultant loss in hard bubble suppression. Low temperatures (473-523 K) cannot achieve this. They do, however, cause a slight increase in H_0, presumably because they increase the permeability of the cap to enhance keepering. With the heavier (2×10^{14}) implants there exists a region of overdamage in which the keepering action is ineffective. Annealing reduces the damage to below the overdamage threshold, thus greatly increasing the cap thickness. The combination of the thicker cap and its increased permeability is responsible for the large increase in H_0.

From the annealing data it is clear that significant changes in the film H_0 will result from device fabrication. Since the magnitude of ΔH_0 depends on the exact temperature, time and number of times the part has to be reworked through a given fabrication step, a preanneal of the implanted film at a temperature above any of the subsequent processing temperatures is one possible way of stabilizing H_0.

Conclusions

During processing of garnet films for magnetic bubble applications, control of the film tolerances, particularly H_0, must be maintained at each stage. Uniformity in H_0 of ±1 percent across 5-cm (2″) wafers can be readily achieved by the LPE film growth process, and excellent film-to-film reproducibility is made possible by the combined efforts of film growth and a post-growth etching treatment. Ion implantation effects are well understood. The short processing times involved and the reproducibility attained readily lend themselves to a manufacturing environment. During post-LPE wafer processing, the elevated temperatures will lead to a significant annealing of the implanted layer with a resulting increase in H_0.

Acknowledgments

The author thanks his colleagues, J. Engemann, G. Galli, E. Giess, J. Suits, H. Turk, and O. Voegeli, for helpful discussion and encouragement; A. Cherry and S. Guerriero for competent technical assistance; and W. C. Ko for ion implanting the films.

References

1. A. H. Bobeck, R. F. Fischer, and J. L. Smith, "An Overview of Magnetic Bubble Domains—Material-Device Interface," *AIP Conf. Proc.* **5**, 45 (1972).
2. S. J. Licht, "Technique for Controlled Adjustment of Bubble Collapse Field in Epitaxial Garnet Films by Etching," *J. Electron Mater.* **4**, 757 (1975).
3. T. Kasai, "Adjustment of Bubble Collapse Field of Garnet Films by Chemical Etching," *Jpn. J. Appl. Phys.* **14**, 1421 (1975).
4. R. Wolfe, J. C. North, R. L. Barns, M. Robinson, and H. J. Levinstein, "Modification of Magnetic Anisotropy in Garnets by Ion Implantation," *Appl. Phys. Lett.* **19**, 298 (1971).
5. H. J. Levinstein, S. Licht, R. W. Landorf, and S. L. Blank, "Growth of High Quality Garnet Thin Films from Supercooled Melt," *Appl. Phys. Lett.* **19**, 486 (1971).
6. E. A. Giess, J. D. Kuptsis, and E. A. D. White, "Liquid Phase Epitaxial Growth of Magnetic Garnet Films by Isothermal Dipping in a Horizontal Plane with Axial Rotation," *J. Cryst. Growth* **16**, 36 (1972).
7. H. L. Turk, IBM General Products Division, San Jose, CA, private communication.

8. B. S. Hewitt, R. D. Pierce, S. L. Blank, and S. Knight, "Technique for Controlling the Properties of Magnetic Garnet Films," *IEEE Trans. Magn.* **MAG-9**, 366 (1973).
9. B. F. Stein, "Growth of Garnet Films by Liquid Phase Epitaxy," *AIP Conf. Proc.* **18,** 48 (1973).
10. T. Kasai and F. Ishida, "Control of the Properties of Magnetic Garnet Films," *Mater. Res. Bull.* **10,** 807 (1975).
11. S. J. Lewis, "Regression Model for LPE Film Property Control," to be published.
12. H. Callen and R. M. Josephs, "Dynamics of Magnetic Bubble Domains with an Application to Wall Velocities," *J. Appl. Phys.* **42,** 1977 (1971).
13. A. Reisman, M. Berkenblit, J. Cuomo, and S. A. Chan, "The Chemical Polishing of Sapphire and Spinel," *J. Electrochem. Soc.* **118,** 1653 (1971).
14. R. Wolfe and J. C. North, "Suppression of Hard Bubbles in Magnetic Garnet Films by Ion Implantation," *Bell Syst. Tech. J.* **51,** 1436 (1972).
15. J. A. Seman, S. H. Wemple, and J. C. North, "Optical Absorption in Ion-Bombarded Magnetic Garnet Films," *J. Appl. Phys.* **45,** 2700 (1974).
16. R. Wolfe and J. C. North, "Planar Domains in Ion-Implanted Magnetic Bubble Garnets Revealed by Ferrofluid," *Appl. Phys. Lett.* **25,** 122 (1974).
17. J. Engemann and T. Hsu, "The Effect of Ion Implantation on the Minimum Bubble Drive Field in Magnetic Garnet Films," *Appl. Phys. Lett.* **30,** 125 (1977).

Received March 25, 1977; revised June 24, 1977

The author is located at the IBM General Products Division laboratory, 5600 Cottle Road, San Jose, California 95193.

B. T. Bennett
P. A. Franaszek

Permutation Clustering: An Approach to On-Line Storage Reorganization

Abstract: A class of dynamic reorganization algorithms is described which embodies a number of desirable systems properties. Experiments on a trace taken from a large data base application indicate that a member of this class may be used to obtain time-varying or quasistatic organizations that exhibit improved paging performance.

Introduction

A memory hierarchy is a storage system composed of a number of levels, $L_1, L_2, \cdots, L_n$, implemented in a variety of device types, whose purpose is to provide an average access time close to that of the fastest, with an average cost per byte approximating that of the slowest, low-cost devices [1]. This performance is achieved by controlling the location of data within the hierarchy as a function of reference patterns. The techniques for such control may be of two kinds: a) replacement policies which determine what information will be kept at each level, and b) clustering methods whose goal is to ensure that accesses to slower portions of the system result in fetches of collections of data likely to be referenced together. This paper presents a systematic approach to the formulation of techniques of the latter kind.

Figure 1 illustrates a three-level storage hierarchy. Here L_1 is the high speed buffer or cache, L_2 is random access main memory, and L_3 is the backing or secondary store, typically implemented by direct access devices such as drums or disks. Each level L_j in such a system has associated with it allocation and replacement policies for units of size U_j, corresponding to a *line* in L_1 and a *page* in L_2. It is common to refer to L_1 as the highest and L_n as the lowest level.

In general, the unit of transfer into a level L_j from below may be regarded as an integer multiple of the replacement unit U_j, where this integer may be larger than one. For example, data may be moved into main memory L_2 from secondary storage in blocks U_3 each of which comprises q_2 pages U_2. The pages in each such block would then be managed as separate units by the L_2 paging policy. Such multiple-page transfers may be regarded as a form of prefetching. Because the cost of transferring a block of q_2 pages that reside in contiguous space on L_3 is considerably less than q_2 times that for a single page, and because the resulting page fault rate may be substantially lower than that for demand paging [2, 3], such a policy may yield attractive benefits.

The performance gains obtainable from a block transfer policy are directly related to the degree to which pages which reside in a block tend to be referenced together. Clustering of pages for this purpose can be performed manually by a programmer familiar with reference patterns, or automatically by the system. Automatic reorganization may be of two kinds: that which is done off line, as in many access methods [4] and some techniques for restructuring programs [5], and that which is done dynamically whenever data is moved to a lower level in the hierarchy. An example of a system which uses a dynamic method is TSS [6], in its policy for migration of data sets between on-line and off-line disks. There have also been suggestions for doing such reorganization when pages are moved between main memory and the backing store [3].

This paper develops a systematic approach to dynamic reorganization. For simplicity, only transfers between main memory and secondary storage are treated, but the approach is readily extensible to other levels. The discussion concentrates on the movement of pages and blocks, objects seen by the system memory management. However, it should be noted that one of the most promising areas for dynamic reorganization is that of large data bases. Here it is data records that are subject to clustering. The experiments described below in fact involve the Advanced Administrative System (AAS) data base [7], where the physical record size is taken to be exactly one page.

The following is a brief summary of the paper. The next section discusses a set of desirable properties for dynamic clustering algorithms in systems where there